The Role of Salt in Governing the Adsorption Mechanisms of Micelle-Forming Polyelectrolyte/Neutral Diblock Copolymers

Ryan Toomey,[⊥,†] Jimmy Mays,[‡,§] and Matthew Tirrell*[,†]

Department of Chemical Engineering and Materials Research Laboratory, University of California at Santa Barbara, Santa Barbara, California 93106; Department of Chemistry, University of Tennessee, Knoxville, Tennessee 37996; and Chemical Sciences Division, Oak Ridge National Laboratory, Oak Ridge, Tennessee 37831

Received May 23, 2005; Revised Manuscript Received October 26, 2005

ABSTRACT: The adsorption kinetics of amphiphilic poly(*tert*-butyl styrene)-*block*-poly(sodium styrenesulfonate) copolymers have been monitored as a function of a monovalent 1:1 salt (sodium chloride) to hydrophobic octadecylsilane (OTS) surfaces and compared to the adsorption kinetics of poly(sodium styrenesulfonate) homopolymer. The initial adsorption rate of the homopolymer shows a weak power-law dependence on the external salt concentration, $\phi_s^{1/10}$, at salt concentrations above 0.01 M, in agreement with diffusion-limited kinetics. Moreover, the adsorbed amount reaches a definitive plateau in less than 24 h at all salt concentrations. The initial adsorption rate of the copolymer, on the other hand, adsorbs 1−2 orders of magnitude more slowly than the homopolymer and does not follow diffusion-limited kinetics, which can be ascribed to the presence of micelles. Micelles adsorb to the surface, but the micelles must overcome a potential energy barrier in order to adsorb. That being said, the copolymer micelles eventually surpass the adsorbed amount of the homopolymer and show no signs of reaching saturation, even after 1 week of adsorption. The copolymer shows two types of adsorption kinetics at long times. If the external salt concentration ϕ_s is sufficiently higher than the counterion concentration associated with the adsorbed layer, the copolymers adsorb with $\phi_s^{2/5}\{\log(t)\}^{6/5}$ kinetics. In the other limit, where the internal ion concentration in the brush layer is higher than the external salt concentration, the adsorption kinetics show weak power-law behavior. Simple scaling relationships have been established to understand the qualitative differences between adsorption in the two regimes.

I. Introduction

Amphiphilic diblock copolymers comprising a polyelectrolyte block and a short hydrophobic tail have long been recognized as excellent anti-flocculation agents, for they can impart a combination of steric and charge stabilization to colloidal systems.[1−5] Interestingly, self-assembled polyelectrolyte motifs may also realize their full potential in the growing field of microfluidics, where surface properties must be precisely controlled in many applications.[6,7] Polyelectrolytes end-grafted to a surface, for instance, have been shown to mediate wetting, lubrication, and biocolloid adhesion.[8] While in situ polymerization has become increasingly pursued in the preparation of end-grafted polyelectrolytes,[9] the adsorption of preformed polymers still remains appealing as self-assembly does not require specially controlled conditions or the preparation of reactive surfaces.[10]

While there have been a few published theories that describe the influence of salt on the equilibrium adsorbed amount for polyelectrolyte diblock copolymers,[11−15] a true test of these theories remains challenging. The precise role that salt plays is quite complex. While in general the addition of salt screens electrostatic repulsions and favors faster adsorption time scales, the addition of salt also favors micellization. Micelles themselves may directly adsorb to the surface; however, the hydrophobic blocks must be sufficiently mobile to permit rearrangement of the micelle once adsorbed. The attainment of thermodynamic equilibrium, in this case, may require unreasonably long equilibration times due to the extremely large potential energy barriers involved.

That being said, equilibrium in the adsorption process is not a necessary requirement for effective modification of surface properties. Layer growth slows resulting from a sufficiently high density that effectively resists further adsorption. The self-limiting aspect of adsorption ensures that interactions between neighboring chains are well developed enough to impart the properties of tethered polymers to the adsorbing surface.

Very little literature exists on the adsorption kinetics of amphiphilic polyelectrolyte/hydrophobic diblock copolymers from aqueous solutions. A recent study by Abraham et al.[15] showed that the plateau adsorbed amount of poly(*tert*-butyl methacrylate)-*b*-poly(glycidyl methacrylate sodium sulfonate) followed a weak 4/23 power-law dependence on sodium chloride concentration and almost no salt dependence on the initial "fast" adsorption regime. In this work, we investigate the adsorption behavior of diblock copolymer poly(*tert*-butyl styrene)-*b*-poly(styrene sodium sulfonate) (PtBS-*b*-NaPSS) micelles and NaPSS homopolymer as a function of a monovalent salt, sodium chloride (NaCl), to address the role of ionic strength on the interfacial assembly of brush layers from micellar solutions. All adsorptions were carried out with hydrophobic OTS surfaces, which are highly selective for the PtBS block, and monitored in situ with phase-modulated ellipsometry.

II. Materials and Methods

Materials. Diblock copolymers of PtBS and NaPSS were produced by sulfonation of a precursor diblock of PtBS and polystyrene (PS), which was prepared by anionic polymerization. The material was selectively sulfonated by the method of Valint

† University of California at Santa Barbara.
‡ University of Tennessee.
§ Oak Ridge National Laboratory.
⊥ Current address: Department of Chemical Engineering, University of South Florida, Tampa, FL 33701.
* Corresponding author. E-mail: tirrell@engineering.ucsb.edu.

10.1021/ma0510542 CCC: $33.50 © 2006 American Chemical Society
Published on Web 12/15/2005

Table 1. Polymer Molecular Characteristics

sample	M_w NaPSS	M_w PtBS	M_w/M_n	% sulfonation[a]	N_{NaPSS}[b]	N_{PtBS}[b]
$NaPSS_{444}$	87 000		1.1	90	444	
$PtBS_{15}$-*b*-$NaPSS_{438}$	86 000	2400	1.05	89	438	15

[a] Sulfonation degree is calculated from the elemental analysis analysis data on sulfur. [b] Weight-average degree of polymerization.

and Block to yield ~90% sulfonation for all samples.[16,17] The sulfonic acid groups were neutralized using sodium methoxide to generate the final diblock copolymers. To preserve their water solubility, all the copolymers were made highly asymmetric with a small hydrophobic PtBS block relative to a large NaPSS block. NaPSS homopolymer of molecular weight 87 000 was purchased from Polysciences and used as received. The molecular characteristics of the polymers are shown in Table 1. Optically clear solutions were obtained by dissolving the polymer in Milli-Q water at a known concentration (100−500 ppm) and stirring for 2−4 weeks. At ~1 week prior to the experiment, the solutions were diluted to the desired concentration and the appropriate amount of sodium chloride was added. At this time, the solutions were gently stirred at 90 °C for 3 days followed by 4 days at room temperature to ensure equilibrium and reproducibility of the solution. Immediately before the experiment, the solutions were filtered through a 0.45 μm polycarbonate filter.

To prepare surfaces for adsorption, (100)-oriented, double-sided polished, test grade silicon wafers (Virginia Semiconductor) were cut into pieces of appropriate size (~1 cm^2) and cleaned by a two-step process. First, they were dipped into a freshly made 70:30 (v/v) sulfuric acid/hydrogen peroxide solution for 10−15 min followed by rinsing under Milli-Q water for 3−5 min. To remove any remaining contaminants, the wafers were exposed to a UV cleaning chamber between 5 and 10 min. The UV light source was a low-pressure mercury quartz lamp. This treatment yields a hydrophilic, contaminant-free surface with a native oxide (SiO_2) layer of 14−15 Å thick, as checked by ellipsometry. Octadecylsilane (OTS) films were made by immersing the substrates in 10^{-3} mol/L solutions of octadecyltrichlorosilane in toluene for 1−2 h. Octadecyltrichlorosilane (Aldrich, 95%) and toluene (Sigma-Aldrich, HPLC grade, 99.8%) were commercially available and used as received. The coating solutions were used for no more than 1−2 days, after which they were discarded and new solutions made. The film-covered substrates were then removed from the solution and baked at 110 °C for 1 h to remove any excess water and drive complete hydrolysis of the OTS layer. If the OTS deposition was successful, the toluene solution will dewet the surface and bead off as the substrate is removed. Following the baking step, the substrates were sonicated in HPLC grade chloroform to remove any loose OTS.

Ellipsometry showed the final film thickness was on the order of 20−22 Å (the contour length of a single molecule is 26 Å); therefore, the surface coverage is on the order of 80%. Typical advancing angles were 110−115° and receding angles were 100−105°. Receding angles of less than 95° indicated a poorly formed layer, and these substrates were discarded.

Ellipsometery Measurements. All adsorption experiments were conducted with a Beaglehole picometer ellipsometer, which uses a He−Ne laser light source ($\lambda = 632.8$ nm), has an angular resolution of 1/100, and is based on phase modulation technique of Jasperson and Schnatterley.[18] The ellipsometer directly measures the real and imaginary components of the ellipsometric ratio[19]

$$\rho = \frac{r_p}{r_s} = \tan \Psi e^{i\Delta} \qquad (1)$$

where $\mathrm{Re}(\rho) = \tan \Psi \cos \Delta$ and $\mathrm{Im}(\rho) = \tan \Psi \sin \Delta$. r_p and r_s are the complex overall reflection coefficients of the p and s polarizations, respectively. The angles Ψ and Δ correspond to the ratio of attenuation of the p and s polarizations and the phase change between the p and s polarizations, respectively.

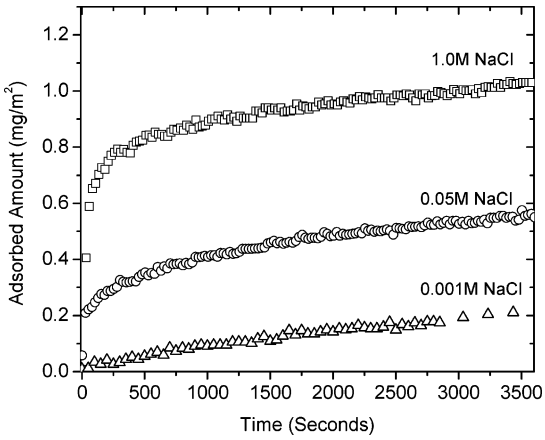

Figure 1. Adsorption of $NaPSS_{442}$ at 100 ppm from NaCl aqueous solution to OTS.

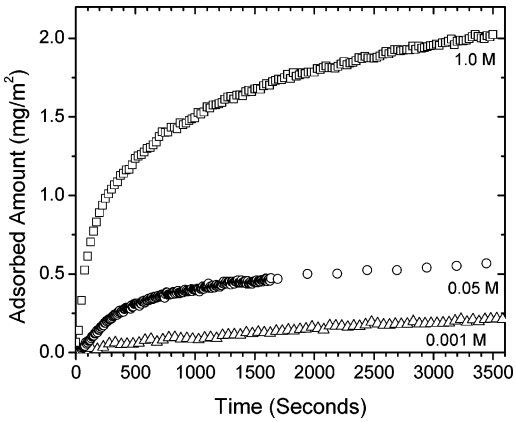

Figure 2. Adsorption of $PtBS_{15}$−$NaPSS_{438}$ at 100 ppm from NaCl aqueous solution to OTS.

At the beginning of the experiment, an OTS/silicon substrate was inserted into a specially built cylindrical solution cell. The cell was then filled with polymer-free solution at the desired salt concentration. The angle of incidence was set at the Brewster angle (~71°) for the water/silicon interface. At this angle, $\Delta = 90°$ and $\mathrm{Im}(\rho) \leq 0.005$. If $\mathrm{Im}(\rho)$ remained constant over the next 15 min, the polymer solution was introduced through the cell inlet. The adsorbed amount Γ (mass/area) was then determined using the following analysis[20]

$$\mathrm{Im}(\rho) - \mathrm{Im}(\rho)_{\mathrm{baseline}} = \frac{2\pi}{\lambda} \frac{\sqrt{n_{\mathrm{solvent}}^2 + n_{\mathrm{substrate}}^2}}{n_{\mathrm{solvent}}} \left(\frac{dn}{dc}\right) \Gamma \qquad (2)$$

where $\lambda = 632.8$ nm, $n_{\mathrm{substrate}} = 3.88$, and $dn/dc = 0.168$ mL/g.[21] The refractive index of the solvent is $1.3327 + 0.009C_{\mathrm{NaCl}}$, where C_{NaCl} is given in units of mol/L. In the range of salt concentrations studied, the refractive index increment of the polymer was found to be relatively independent of salt concentration. The refractive index increment dn/dc for the copolymers was measured with a standard Abbe refractometer. The dn/dc values of both the NaPSS homopolymer and the NaPSS/PtBS diblock copolymers were approximately the same due to the relatively small size of the PtBS blocks.

III. Results and Discussion

Both $NaPSS_{442}$ homopolymer and $NaPSS_{438}$−$PtBS_{15}$ diblock copolymers were adsorbed to neutral hydrophobic OTS surfaces over a range of sodium chloride concentrations, from 0.001 to 1 M, as shown in Figures 1 and 2, respectively. The bulk polymer concentration in each experiment was 100 ppm. As expected, the external salt concentration plays an important role

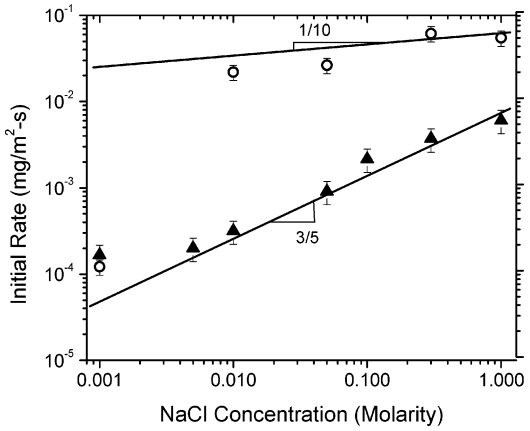

Figure 3. Initial adsorption rate of $NaPSS_{442}$ homopolymer (○) and $PtBS_{14}-PSS_{438}$ diblock copolymers (▲) at a polymer concentration of 100 ppm onto OTS surfaces.

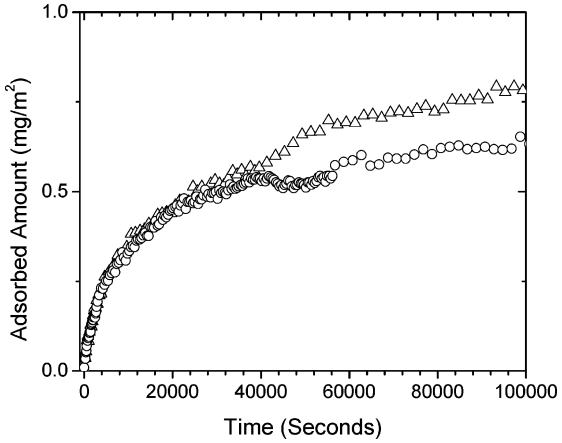

Figure 4. Comparison of $NaPSS_{422}$ homopolymer (○) and $PtBS_{14}-NaPSS_{438}$ diblock copolymer (△) at a polymer concentration of 100 ppm and 0.001 M NaCl.

in the formation rate of the adsorbing layer. Figure 3 shows the initial adsorption rates $d\Gamma/dt_0$ for both the homopolymer and copolymer. The symbol Γ refers to the adsorbed amount, and t is time. For all experiments, the initial rate was averaged over the first 0.005 mg/m^2 of adsorption. While such averaging does not reveal the true adsorption rate at zero time, there generally was too much scatter in the data at lower adsorbed amounts to determine the initial value reliably.

Despite the scatter in rate determination data, the trends in the averaged initial adsorption rate for the homopolymer and the copolymer are quite striking. At the lowest salt concentration (10^{-3} M), the initial population rate by both the block copolymer and the homopolymer are approximately the same. As the salt concentration is increased, the initial adsorption rate of the homopolymer quickly supersedes the copolymer. At the highest salt concentration, 1 M NaCl, the homopolymer adsorbs nearly an order of magnitude faster than the copolymer.

For flexible polyelectrolytes under dilute conditions and moderate salt concentrations, the radius of gyration R_g scales with the salt concentration C_s as $R_g \propto C_s^{-1/5}$.[22] The diffusion coefficient D is inversely proportional to the coil radius, and therefore the diffusion coefficient scales as $D \propto C_s^{1/5}$. For bulk diffusion-limited adsorption, the adsorbed amount Γ increases with square-root time kinetics[11,23,24]

$$\Gamma(t) = C_B\sqrt{\frac{4Dt}{\pi}} \tag{3}$$

Therefore, the averaged adsorption rate at the beginning of the experiment should be weakly dependent on the salt concentration, following a $C_s^{1/10}$ power law. This predicted power law describes the adsorption rate of homopolymer above 0.01 M to at least 1.0 M NaCl rather well, as shown in Figure 3.

At the lowest salt concentration 0.001 M, a strong deviation from bulk-diffusion-limited adsorption is observed, which probably originates from the entropic penalty of localizing counterions within the interfacial zone. The excess surface charge per unit of adsorption $\sigma f N_a$ defines the so-called Gouy−Chapman length λ:[1,25]

$$\lambda = (2\pi l_B N_A f\sigma)^{-1} \tag{4}$$

where l_B is the Bjerrum length, N_a is the degree of polymerization of the polyelectrolyte block, f is the charged fraction, and σ is the number of chains per unit area. For the NaPSS chains used in this study, f can be approximated as nearly unity, or $f = 1$. The Guoy−Chapman length is the width of the region over which the counterions balance the surface charge of the adsorbed layer. In the start of the adsorption experiment, $\lambda > \kappa^{-1}$ and bulk diffusion of the individual chains to the surface dominates. As the adsorbed amount Γ increases, the counterion cloud is pulled closer to the surface, and eventually the Debye screening length κ^{-1} supersedes the Gouy−Chapman length λ. At this point, a significant barrier to adsorption develops, for the osmotic pressure of the interfacial counterions now exceeds the bulk value. At 0.001 M, the Debye screening length κ^{-1} is 96 Å. The adsorbed amount of a layer that corresponds to the Guoy−Chapman length λ of the same value is 0.0085 mg/m^2. Therefore, it could be expected that at 0.001 M a significant adsorption barrier exists even in the initial stages of adsorption, and diffusion-limited adsorption cannot be experimentally observed. As the external salt is raised an order of magnitude to 0.01 M, $\kappa^{-1} = 30$ Å, which corresponds to an adsorbed amount of 0.028 mg/m^2. Presumably, at a salt concentration of 0.01 M and above, the ionic strength is now sufficiently high to permit diffusion-limited kinetics to dominate in the beginning of the experiment.

The initial adsorption rate of the block copolymer, in contrast to the homopolymer, follows an approximately 3/5 power-law dependence on salt between 0.0001 and 1.0 M. The initial overlap of the homopolymer and copolymer adsorption trajectories at 0.001 M (Figure 4) suggests that at 0.001 M the copolymer chains exist primarily in a nonaggregated state and adsorb in the same manner as the homopolymer chains. As the salt concentration is increased, it is known that the copolymer forms micelles,[26] and therefore the slower adsorption rates of the copolymer can be attributed to micelle adsorption. Figure 5 compares the adsorption trajectories of the copolymer and the homopolymer at 1.0 M NaCl.

To determine whether the rate of micelle adsorption is diffusion limited, the relationship between the radius of the micelle and salt concentration must be known. Assuming that the salt concentration is sufficiently high, the micelle can be modeled as a star copolymer comprising close-packed excluded-volume blobs. The Daoud−Cotton model for star polymer with p arms states that the correlation length of a blob ξ is a monotonically decreasing function of the radius r: $\xi \sim r/p^{1/2}$. For flexible polyelectrolytes in the semidilute regime, the excluded-volume correlation length ξ scales as[27]

$$\xi \approx a^{-1/2}\frac{\phi_s^{1/4}}{\phi^{3/4}} \tag{5}$$

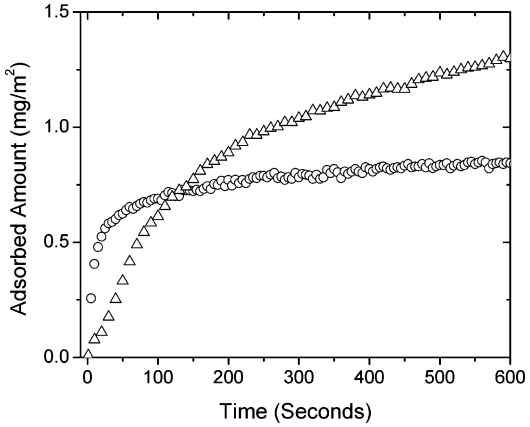

Figure 5. Comparison of $NaPSS_{422}$ homopolymer (○) and $PtBS_{14}$−$NaPSS_{438}$ diblock copolymer (△) at a polymer concentration of 100 ppm and 1.0 M NaCl.

where a is the segment length, ϕ_s is the salt concentration, and ϕ is the polymer chain concentration. Combination of the Daoud−Cotton model with eq 5, the relationship between the local segment concentration a distance r from the center, is

$$\phi(r) \approx a^{-2} p^{2/3} \phi_s^{1/3} \left(\frac{r}{a}\right)^{-4/3} \tag{6}$$

The size of the star R is determined by the stipulation that the integral of the segment concentration equals the total number of segments N_a. In other words

$$pN_a a = \int r^2 \phi(r)\, dr \tag{7}$$

and

$$R_{star} = a^{2/5} N_a^{3/5} p^{1/5} \phi_s^{-1/5} \tag{8}$$

If the aggregation number p is weakly dependent on the salt concentration, the radius of a micelle scales with the same salt dependence as a single chain, and it would be expected that the initial adsorption rate of the two systems would also have the same salt dependence. The departure of the initial adsorption rate of the copolymer from a $C_s^{1/10}$ power law, therefore, could stem from one of two explanations: either the aggregation number of the micelles is a strong function of the salt concentration or the micelles themselves do not adsorb according to diffusion-limited kinetics. If we take the former explanation to be true, the aggregation number of the micelle would have to scale as C_s^{-5} to be consistent with the initial adsorption rate, which is probably an unreasonable assumption. Furthermore, the initial rate of copolymer adsorption is at least 1 order of magnitude slower than the homopolymer. To be consistent with diffusion-limited kinetics, the size of the copolymer micelles would have to be at least 2 orders of magnitude larger than their constituent chains, which is also an unreasonable assumption. These two bits of information lead us to believe that micelle adsorption is not a diffusion-limited process, but rather micelles must overcome a potential energy barrier in order to adsorb, consistent with previous observations.[28] In reality, micelle adsorption would not be necessarily expected to follow a simple power-law behavior for a number of reasons. The critical micelle concentration, aggregation number, and polydisperity of the aggregates are expected to depend on the salt concentration.[29] Therefore, it is perhaps coincidental that the initial rate of the adsorption of the PtBS−NaPSS copolymers shows power-law-like behavior over the experimental range of salt concentrations.

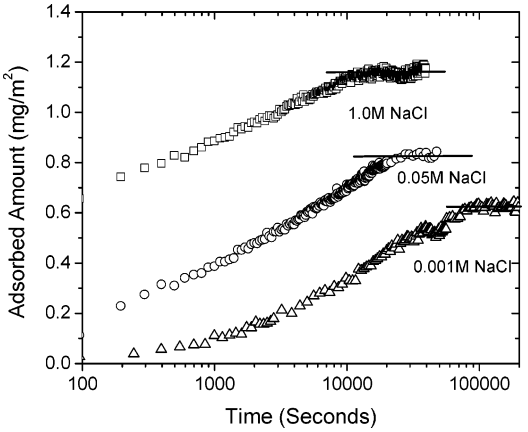

Figure 6. Linear−log plot showing the long-term adsorption behavior of $NaPSS_{422}$ at 100 ppm from aqueous solution.

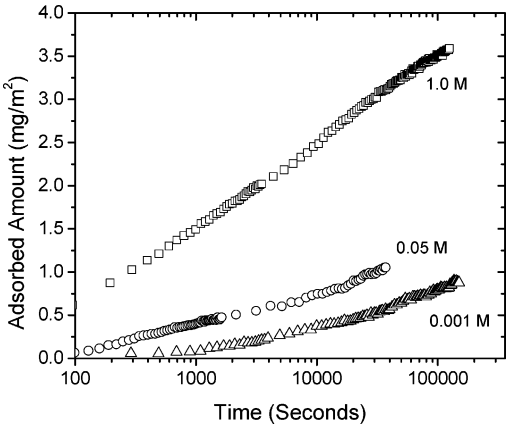

Figure 7. Adsorption of $PtBS_{15}$−$NaPSS_{422}$ at 100 ppm from NaCl aqueous solution to OTS.

Despite the fact that the PtBS−NaPSS copolymer initially adsorbs more slowly than the homopolymer at salt concentrations above 0.001 M, the copolymers consistently generate adsorbed layers with much higher surface coverages than the NaPSS homopolymers. The long-time adsorption behavior of both the homopolymer and copolymer is shown in Figures 6 and 7, respectively. In every case, the homopolymer achieves a clear plateau in the adsorbed amount whereas the copolymer does not. At the highest salt concentration, 1.0 M NaCl, the homopolymer reaches a plateau value of 1.2 mg/m^2 in 3 h. The block copolymer achieves 2.5 mg/m^2 in the same time and shows a persistent growth rate that is approximately logarithmic in time. Likewise, adsorption of the copolymer at 0.05 M and the 0.001 M NaCl show no evidence of a plateau in the adsorbed amount.

In fact, adsorption of the copolymer was conducted for up to several days, but no definitive plateau in the adsorbed amount was found. The adsorption of PtBS−NaPSS at an ionic strength of 1.0 and 0.001 M sodium chloride was allowed to continue until ∼3.0 mg/m^2 was achieved, as shown in Figure 8. The 1.0 M system reaches 3.0 mg/m^2 in ∼50 h, and by observing the trajectory of the adsorption curve, it can be seen that adsorption is probably far from complete. Amazingly, the 0.001 M system also reaches 3.0 mg/m^2, but on a much slower time scale (450 h). Another striking difference is the difference in shape of the adsorption curves at low and high salt. Whereas the adsorption at 1.0 M is almost linear with respect to log(t), the 0.001 M case displays weak power law behavior with respect to time.

To at least qualitatively understand the differences in the adsorption kinetics between the two cases, it is necessary to

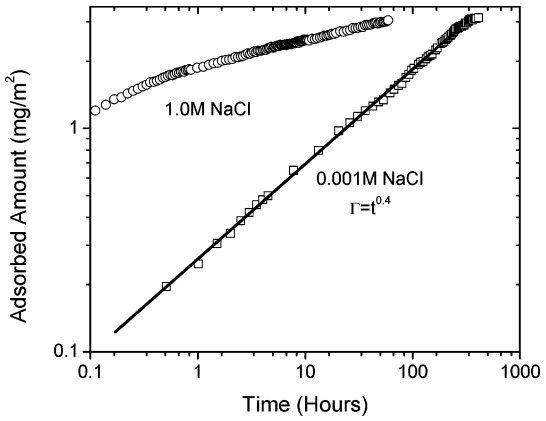

Figure 8. Long-term adsorption of $PtBS_{15}-NaPSS_{422}$ at 100 ppm from NaCl aqueous solution to OTS. Adsorption from a 0.001 M NaCl leads to power-law kinetics with a weak value of the power-law exponent.

understand the principal contribution to the barrier resistance at low and high salt. This can done along the lines of the approach taken by Semenov and Joanny using the Kramers equation to determine the adsorption rate constant K[30,31]

$$K^{-1} = \int \frac{1}{D} e^{u(\Gamma,z^*)/kT} dz^* \tag{9}$$

where $u(\Gamma,z^*)$ is the potential felt by the adsorbing species a distance z^* from the surface. The adsorption rate is expressed as

$$\frac{d\sigma}{dt} = K\phi_B \tag{10}$$

where ϕ_B is the bulk polymer concentration. The nature of the potential u depends on whether the counterion concentration associated with the adsorbed layer ϕ_i is larger than the bulk ion concentration in solution ϕ_s. The average ion concentration associated with the brush is

$$\phi_i = \frac{N_A \sigma}{L} \tag{11}$$

where L is the thickness of the adsorbed layer. If the counterion density due to the grafted chains is smaller than the external salt concentration, the osmotic pressure Π of the adsorbed layer is dictated by polymer−polymer contacts and scales as $\phi^{9/4}$.[32] In this regime, the free energy of a tethered polymer chain is determined by the number of excluded-volume blobs that comprise the layer, $kT(L/\xi)$. The correlation length is set by the graft density, $\xi = \sigma^{-1/2}$, and the thickness of a brush is $L = a^{2/3}N_a\sigma^{1/3}\phi_s^{-1/3}$.[1] The potential that a chain must overcome in order to adsorb is

$$\frac{u_{salted}}{kT} = \frac{L}{\xi} = a^{2/3}N_a\sigma^{5/6}\phi_s^{-1/3} \tag{12}$$

Assuming a uniform density profile, the diffusive motion is expressed as $D = kT(6\pi\eta\xi)^{-1}$ and the rate constant can be expressed as

$$K = \frac{kT\sigma^{1/6}\phi_s^{1/3}}{6\pi\eta N_A a^{2/3}} \exp(-a^{2/3}N_A\sigma^{5/6}\phi_s^{-1/3}) \tag{13}$$

Insertion of the expression of K into eq 10 can be integrated to yield

$$\sigma(t) = \phi_s^{2/5} a^{-4/5} N_A^{-6/5} \ln\{(t\phi_B kT/6\pi\eta)\}^{6/5} \tag{14}$$

In the low salt limit, where the counterion concentration in the adsorbed brush layer is greater than the bulk ion concentration, Pincus suggested that the osmotic pressure of the brush is dominated by the counterion osmotic pressure.[1] In this limit, the potential required for a chain to be inserted into the layer can be expressed as[25]

$$u_{osmotic} = kTN_a \ln\left(\frac{\phi_i}{\phi_s}\right) \tag{15}$$

In the limit of low salt, no agreed upon scaling regime exists for the diffusion coefficient of a single polyelectrolyte chain, if one even exists.[33] However, because of the logarithm in the osmotic barrier term, the adsorption rate constant K will have a form that resembles

$$K \propto \left(\frac{\phi_i}{\phi_s}\right)^{-N_A} \tag{16}$$

When inserted into the rate law in eq 10, the adsorption rate can be expressed as (for large values of N_A)

$$\sigma(t) \propto \phi_s(tN_A\phi_B)^{1/N_A} \tag{17}$$

Equations 14 and 17 provide a phenomenological relationship between the external salt concentration and the adsorption kinetics of the NaPSS block copolymer at long times. More generally, the relations suggest that the adsorption will cross over from a $\{\log(t)\}^{6/5}$ dependence to a very weak power-law dependence at the point when the counterion concentration in the adsorbed layer starts to supersede the external salt concentration.

Plotting the adsorption kinetics of the block copolymer as $\Gamma/\phi_s^{2/5}$ vs $\{\log(t)\}^{6/5}$ reveals the applicability of the rate equation (eq 14) at high salt concentrations. Both the 0.05 and 1.0 M adsorption trajectories show remarkable overlap when plotted as the reduced variable $\Gamma/\phi_s^{2/5}$, and they both follow $\{\log(t)\}^{6/5}$ kinetics. Adsorption at 0.001 M, on the other hand, shows a deviation from $\{\log(t)\}^{6/5}$ kinetics early into the adsorption process, a strong indication that the counterion concentration in the adsorbed layer is greater than the external salt concentration for most of the adsorption process. The large value of the power law in eq 17 would seem to preclude adsorption altogether in this regime; however, perhaps a strong hydrophobic interaction between the adsorbing species and surface helps to overcome the counterion osmotic barrier.[34] It must be empha-

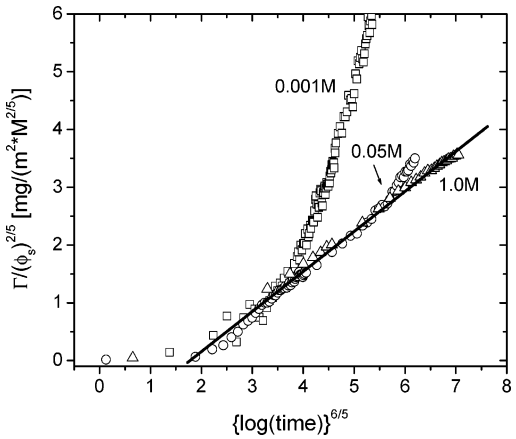

Figure 9. Adsorption of $PtBS_{15}-NaPSS_{422}$ at 100 ppm from NaCl aqueous solution to OTS.

sized that the potential barrier used in the rate equations only applies to the adsorption of single chains. Nevertheless, a recalculation of the potential barrier for a micelle with p chains may not be necessary as long as p is very weakly dependent on the salt concentration and the effective adsorbing concentration is much larger than the cmc, or the critical micelle concentration. On the other hand, if either p depends strongly on the salt concentration or if the adsorbing concentration is near the cmc, the potential barrier must be more rigorously calculated to correctly capture the correct dependence of the adsorption rate on the salt concentration.

IV. Conclusions

We have examined how PtBS-*b*-NaPSS copolymers adsorb under the influence of a monovalent 1:1 salt. Over the range of salt concentrations studied (3 orders of magnitude), the block copolymers consistently produced surface coverages that were higher than the corresponding NaPSS homopolymer, despite solution association effects in the block copolymer. Moreover, the block copolymers show no sign of plateau behavior in the adsorption process, as opposed to the homopolymers, which tend to saturate within a day. This observation indicates that adsorbed micelles are capable of relaxing and reorganizing, however slow this rearrangement may be. The reorganization favors an efficient "end-tethered" packing arrangement that permits higher adsorbed amounts than can be achieved by homopolymers. Depending on the amount of excess salt, the adsorption kinetics of the copolymers transition from a $\{\log(t)\}^{6/5}$ dependence to a weak power-law dependence, in agreement with simple phenomenological arguments describing the nature of the potential barrier. The potential barrier, however, was derived assuming thermodynamic equilibrium, and it remains uncertain whether the adsorption kinetics of micelles can be truly described using thermodynamic arguments. While the data suggest that micelles are capable of adsorbing, it is not clear *how* micelles adsorb, whether micelles undergo fission and essentially break up in the interfacial zone or whether micelles adsorb as hemi-micelles and slowly rearrange after adsorption.

Acknowledgment. This work was supported by the NIRT and MRSEC Program of the National Science Foundation under Awards CTS-0103516 and DMR-0080034.

References and Notes

(1) Pincus, P. *Macromolecules* **1991**, *24*, 2912−2919.
(2) Israels, R.; Leermakers, F. A. M.; Fleer, G. J. *Macromolecules* **1995**, *28*, 1626−1634.
(3) Israels, R.; Leermakers, F. A. M.; Fleer, G. J.; Zhulina, E. B. *Macromolecules* **1994**, *27*, 3249−3261.
(4) Israels, R.; Scheutjens, J.; Fleer, G. J. *Macromolecules* **1993**, *26*, 5405−5413.
(5) Balastre, M.; Li, F.; Schorr, P.; Yang, J.; Mays, J. W.; Tirrell, M. *Macromolecules* **2002**, *35*, 9480−9486.
(6) Belder, D.; Ludwig, M. *Electrophoresis* **2003**, *24*, 3595−3606.
(7) Sia, S. K.; Whitesides, G. M. *Electrophoresis* **2003**, *24*, 3563−3576.
(8) Raviv, U.; Giasson, S.; Kampf, N.; Gohy, J. F.; Jerome, R.; Klein, J. *Nature (London)* **2003**, *425*, 163−165.
(9) Prucker, O.; Ruhe, J. *Langmuir* **1998**, *14*, 6893−6898.
(10) Hadziioannou, G.; Patel, S.; Granick, S.; Tirrell, M. *J. Am. Chem. Soc.* **1986**, *108*, 2869−2876.
(11) Amiel, C.; Sikka, M.; Schneider, J. W.; Tsao, Y. H.; Tirrell, M.; Mays, J. W. *Macromolecules* **1995**, *28*, 3125−3134.
(12) Zhang, Y.; Tirrell, M.; Mays, J. W. *Rev. Inst. Fr. Pet.* **1997**, *52*, 177−181.
(13) Zhang, Y. Y.; Tirrell, M.; Mays, J. W. *Macromolecules* **1996**, *29*, 7299−7301.
(14) Abraham, T. *Polymer* **2002**, *43*, 849−855.
(15) Abraham, T.; Giasson, S.; Gohy, J. F.; Jerome, R.; Muller, B.; Stamm, M. *Macromolecules* **2000**, *33*, 6051−6059.
(16) Valint, P. L.; Bock, J. *Macromolecules* **1988**, *21*, 175−179.
(17) Yang, J. C.; Mays, J. W. *Macromolecules* **2002**, *35*, 3433−3438.
(18) Jasperson, S.; Schnatterly, S. *Rev. Sci. Instrum.* **1969**, *40*, 761.
(19) Azzam, R. M.; Bashara, N. M. *Ellipsometry and Polarized Light*; North-Holland Publication: Amsterdam, 1979.
(20) Toomey, R.; Mays, J.; Tirrell, M. *Macromolecules* **2004**, *37*, 905−911.
(21) Zhang, Y. Y. Ph.D. Thesis, University of Minnesota, 1996.
(22) Wang, L. X.; Yu, H. *Macromolecules* **1988**, *21*, 3498−3501.
(23) Johner, A.; Joanny, J. F. *Macromolecules* **1990**, *23*, 5299−5311.
(24) Motschmann, H.; Stamm, M.; Toprakcioglu, C. *Macromolecules* **1991**, *24*, 3681−3688.
(25) Wittmer, J.; Joanny, J. F. *Macromolecules* **1993**, *26*, 2691−2697.
(26) Guenoun, P.; Davis, H. T.; Tirrell, M.; Mays, J. W. *Macromolecules* **1996**, *29*, 3965−3969.
(27) Barrat, J. L.; Joanny, J. F. *Adv. Chem. Phys.* **1996**, *94*, 1−66.
(28) Toomey, R.; Mays, J.; Holley, D. W.; Tirrell, M. *Macromolecules* **2005**, *38*, 5137−5143.
(29) Borisov, O. V.; Zhulina, E. B. *Macromolecules* **2002**, *35*, 4472−4480.
(30) Semenov, A. N.; Joanny, J. F. *J. Phys. II* **1995**, *5*, 859−876.
(31) Stuart, M. A. C.; Hoogendam, C. W.; deKeizer, A. *J. Phys.: Condens. Matter* **1997**, *9*, 7767−7783.
(32) Wang, L. X.; Bloomfield, V. A. *Macromolecules* **1990**, *23*, 194−199.
(33) Chang, R. W.; Yethiraj, A. *J. Chem. Phys.* **2002**, *116*, 5284−5298.
(34) Israelachvili, J. *Intramolecular and Surface Forces*; Academic Press: London, 1992.

MA0510542